SASEC2015
Third Southern African Solar Energy Conference
11 – 13 May 2015
Kruger National Park, South Africa

NUMERICAL INVESTIGATION OF THE EFFECT OF SLOPE ERRORS AND SPECULARITY ERRORS ON THE THERMAL PERFORMANCE OF A SOLAR PARABOLIC TROUGH COLLECTOR SYSTEM

Mwesigye A.[1, 2,*], Bello-Ochende T.[3] and Meyer J.P.[1]
*Author for correspondence
[1]Department of Mechanical and Aeronautical Engineering,
University of Pretoria, Pretoria, 0002, South Africa,
[2]Department of Mechanical Engineering, Tshwane University of Technology,
Private Bag X 680, Pretoria, 0001, South Africa,
[3]Department of Mechanical Engineering, University of Cape Town,
Private Bag X3, Rondebosch 7701, South Africa,
E-mail: mwesigyea@tut.ac.za

ABSTRACT

The optical efficiency of a parabolic trough collector is one of the most important parameters that affect the performance of the entire collector system. In this study, an optical and thermal analysis of a parabolic trough collector system for different slope errors and specularity errors is presented. For optical analysis, the influence of slope errors, specularity errors and system geometry on heat flux distribution on the receiver's absorber tube is determined using Monte-Carlo ray tracing in SolTrace. The ray tracing results are then coupled with a computational fluid dynamics code to investigate the thermal performance of the receiver. Results show that the slope and specularity errors influence the heat flux distribution on the receiver's absorber tube. The optical efficiency of the collector is shown to reduce significantly as the slope errors increase and slightly as specularity errors increase. The influence of slope errors and specularity errors on the thermal performance of the entire system is investigated numerically and presented.

INTRODUCTION

Solar energy is one of the renewable energy resources that is widely available with enormous potential to meet a significant part of the world's energy demand [1]. The parabolic trough technology is the most commercially and technically developed of the concentrated solar power technologies available today. Significant research and development efforts are still underway to further reduce the cost of electricity from these systems and make these systems cost competitive with fossil based electricity [2].

The optical performance of the collector system significantly influences the performance of the entire system. The optical efficiency of the collector depends on several factors which include collector dimensions, angle of incidence and the intercept factor [3]. The intercept factor is the ratio of energy intercepted by the receiver to the energy reflected by the concentrating collector. Pottler *et al.*[4] suggest that intercept factors in the range 96 – 99 % are achievable with appropriate collector design, quality components, proper assembly and installation of the collector. In their study, quality control measures to ensure high values of intercept factors are discussed.

The optical efficiency of the collector is given by [3]

$$\eta_o = \left[K(\theta)\right]\left[\rho(\tau_g\alpha)_n\right]\gamma \quad (1)$$

The factors affecting the optical efficiency can be clearly identified from equation (1). The first bracketed term is the effect from the angle of incidence, the second bracketed term represents the material properties and the last term incorporates all the optical errors. The first term applies when the angle of incidence is not zero, for a fully tracking collector, the material properties and intercept factor are the major factors determining the optical performance of the parabolic trough system.

Gaul and Rabl [5] presented experimental data as well as analytical expressions for the determination of the incidence angle effects on the performance of the parabolic trough receiver. Güven and Bannerot [3] give a detailed illustration of the different types of errors that are likely to be encountered in parabolic trough collectors. These include: (1) Material errors that include the specularirty of the reflective material. (2) Manufacture and assembly errors that include local slope errors, profile errors, misalignment of the reflector during assembly and mislocation of the receiver tube. (3) Operation errors that include tracking errors, errors due to wind loading and temperature effects, reduced specularity due to dust accumulation, misalignment of the receiver during operation due to sagging of the receiver tube, permanent expansion of the

receiver tube and change in location of the effective focus due to increased profile errors.

NOMENCLATURE

a	[m]	Collector aperture width
A_a	[m^2]	Projected aperture area
A_r	[m^2]	Projected absorber tube area
C_R	[-]	Concentration ratio = A_a/A_r
I_b	[W/m^2]	Direct normal irradiance
d	[m]	Diameter
f	[m]	Collector focal length
h	[W/m^2 K]	Convective heat transfer coefficient
k	[W/mK]	Thermal conductivity
$K[\theta]$	[-]	Incidence angle modifier
L	[L]	Length
LCR	[-]	Local concentration ratio
Q_{loss}	[W]	Receiver thermal loss
Re	[-]	Reynolds number
T	[K]	Temperature
V_w	[m/s]	Wind velocity
x	[m]	Cartesian axis direction
y	[m]	Cartesian axis direction

Greek symbols

α	[-]	Absorptivity
ρ	[-]	Collector reflectance
φ_r	[degrees]	Collector rim angle
γ	[-]	Intercept factor
ϑ	[W/m^{2}K^4]	Stefan Boltzmann constant
σ_{slope}	[mrad]	Slope errors
σ_{mirror}	[mrad]	Specularity error
σ_{sun}	[mrad]	Sun error
σ_{track}	[mrad]	Tracking error
σ_{total}	[mrad]	Total error
θ	[degrees]	Receiver circumferential angle
ε	[-]	Emissivity
η_o	[-]	Optical efficiency
η_{th}	[-]	Collector thermal efficiency
τ_g	[-]	Glass cover transmissivity

Subscripts

amb	Ambient state
gi	Glass cover inner wall
go	Glass cover outer wall
ri	Absorber tube inner wall
ro	Absorber tube outer wall
sky	Sky temperature
tot	Total value

Thomas and Guven [6] presented analytical results for the determination of the effect of optical errors on heat flux distribution around the absorber tube of a parabolic trough concentrator. Several other studies have been carried out to investigate the errors affecting the optical performance of parabolic trough systems [6-10].

For quality control purposes, the intercept factor can be measured and necessary improvements made [4]. Moreover, with improvements in the manufacture of these systems, most of the mentioned errors can be minimised. Wendelin [11] present the results of parabolic trough video scanning Hartmann optical tester (VSHOT) optical characterization for different systems. Using space frames from different suppliers, the average rms slope errors ranged from as high as 4.46 mrad to about 3.0 mrad.

Regarding receiver thermal performance, several studies are available in literature on the thermal performance of parabolic trough receivers [12-14]. In these studies and most of the studies available in literature, the detailed influence of these errors on the thermal performance of the parabolic trough system is not presented. Therefore, the focus of this study is to numerically investigate the optical and thermal analysis of parabolic trough collectors at different slope and specular errors. This study focuses on the optical analysis and determination of heat flux distribution in an optical modelling software, SolTrace [15] and the coupling of the obtained heat flux profiles with computational fluid dynamics tool to investigate the thermal performance.

PHYSICAL MODEL

Figure 1(a) shows the 3-D model of a parabolic trough collector system under consideration. Figure 1(b) shows the cross-section view of the parabolic trough receiver. Figure 2 shows the cross-section view of the parabolic trough collector together with the receiver and a trace of some of the incident rays. The geometry of the collector is defined by

$$y^2 = 4fx \tag{2}$$

The focal length is related to the rim angle and aperture width as

$$f = a/4\tan(\varphi_r/2) \tag{3}$$

Where a is the aperture width, f the focal length and φ_r the rim angle. From equations (2) and (3), the geometry of the collector can be fully defined given any two parameters. The concentration ratio used in this study relates the projected area of the collector to the projected area of the absorber tube as $C_R = A_a/A_r$. The other equations that define the geometry of the collector, receiver and the minimum size required to intercept the sun's image are given in Duffie and Beckman [16].

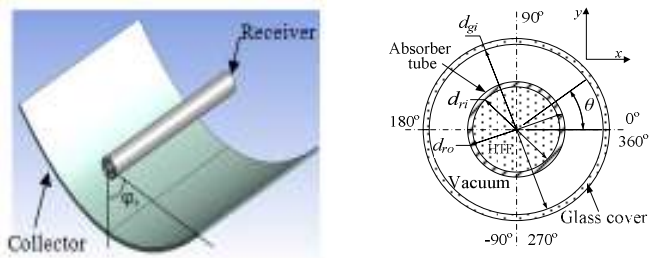

(a) (b)

Figure 1 (a) 3-D model of parabolic trough collector (b) cross-section view of the receiver

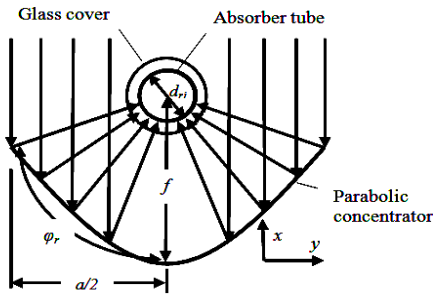

Figure 2 Cross-section view of a parabolic trough collector

THEORETICAL ANALYSIS

For optical analysis of the parabolic trough collectors, the determination of geometrical errors and the influence of these errors on system performance is essential. A commonly used, straight forward and accurate method is statistical ray tracing [17]. In this approach, normal distribution functions of angular deviations from perfect optics are used to describe all kinds of errors [4]. The optical errors are represented as normal probability distributions. The total error is given by [3]

$$\sigma_{tot}^2 = \sigma_{sun}^2 + 4\sigma_{slope}^2 + \sigma_{track}^2 + \sigma_{mirror}^2 \quad (4)$$

Where σ_{sun} represents the standard deviation of the sun's energy distribution, σ_{slope} is the slope error distribution, σ_{track} is the tracking error distribution and σ_{mirror} is the specularity error distribution. These errors are random in nature and are accurately represented by normal (probability distributions) [3].

Non-random errors are deterministic in nature and can degrade the collector performance significantly. They are mainly gross errors in manufacture, assembly and operation of the collector. They include reflector profile errors, consistent misalignment of the collector with the sun, and misalignment of the receiver with the effective focus of the sun. In this study, it is assumed that quality control measures are in place to reduce the non-random errors significantly and therefore their impact on the optical performance of the system is minimal. Further still, the tracking errors and sun errors are also assumed small compared to the slope and mirror errors

For thermal analysis of the receiver, the receiver's annulus space was considered evacuated to very low pressures (about 0.013 Pa) [2]. The receiver's absorber tube has an outer wall that is coated with a cermet selective coating. For a receiver with an evacuated glass envelope such as the ones used in conventional parabolic trough plants, the receiver thermal loss can be obtained as detailed in Duffie and Beckman [16] as

$$Q_{loss} = \frac{2\pi k_{eff,air} L}{\ln \frac{d_{gi}}{d_{ro}}}\left(T_{ro} - T_{gi}\right) + \frac{\pi d_{ro} L \vartheta \left(T_{ro}^{\ 4} - T_{gi}^{\ 4}\right)}{\frac{1}{\varepsilon_{ro}} + \frac{1-\varepsilon_{gi}}{\varepsilon_{gi}}\left(\frac{d_{ro}}{d_{gi}}\right)} \quad (5)$$

Equation (5) gives the thermal loss from the absorber tube to the glass cover. $k_{eff,air}$ is the effective thermal conductivity of air depending on the pressure in the annulus space. An energy balance easily shows that the thermal loss in equation (5) is equivalent to the heat loss from the glass cover to the surroundings.

The emissivity of the glass is taken to be constant and is given as ε_{gi} = 0.86 [18]. The absorber tube emissivity is temperature dependent. For an absorber tube with a cermet selective coating, the emissivity is given as ε_{ro} = 0.000327(T_{ro}+273.15) – 0.065971 [18]. The thermal efficiency, which is the ratio of the useful energy delivered to the incident radiation is given by:

$$\eta_{th} = q_u / I_b A_a \quad (6)$$

The useful energy q_u is the difference between the incident solar energy and the receiver thermal loss.

SOLUTION METHOD

In this study a combined Monte-Carlo ray trace and computational fluid dynamics approach was used. The sections below give the solution procedure used.

Ray Tracing

To investigate the effect of slope errors and specularity errors on heat flux distribution, Monte-Carlo ray tracing was used. The Monte-Carlo ray tracing methodology is implemented in an optical modelling tool SolTrace[15]. This involves specification of the sun shape taken as pillbox in this study, then the geometry of the parabolic trough system, which is obtained by using equation (2) and equation (3), then the optical properties of each of the components of the parabolic trough system. A maximum number of rays from the sun is specified and traced as it goes through several interactions with the different components of the collector system. From this, the distribution of heat flux on the receiver's absorber tube is obtained.

Boundary Conditions

The boundary conditions used in this study were: (1) Non-uniform heat flux on the absorber tube's outer wall determined using ray tracing in SolTrace [15]. A direct normal irradiance (DNI) of 1000 W/m^2 was assumed throughout this work. (2) Velocity inlet and pressure outlet boundary conditions were used for the absorber tube's inlet and outlet respectively. (3) No-slip and no-penetration boundary condition was specified for the inner absorber tube wall. (4) For the inlet and outlet of the receiver's annulus space, a symmetry boundary condition was used such that the normal gradients of all flow variables are zero. (5) On the outer wall of the glass cover, a mixed boundary condition is used to account for both radiation and convection heat transfer. Stefan Boltzmann's law gives radiation between the glass cover and the sky. The sky is taken as a large enclosure. Convection heat transfer from the receiver's glass was modelled by specifying a convection heat transfer coefficient and free stream temperature. The sky temperature is given by $T_{sky} = 0.0552T_{amb}^{1.5}$ [19] while the wind heat transfer coefficient is given by $h_w = V_w^{0.58} d_{go}^{-0.42}$ [20]. The ambient temperature (T_{amb}) was kept at 300 K and the wind speed (V_w) was fixed at 2 m/s. Table 1, shows the summary of the other parameters used in this study.

Table 1. Geometrical and optical values of the parabolic trough collector used in this study

Parameter	Value	Parameter	Value
a	6 m	d_{ri}	0.066 m
L	5 m	d_{ro}	0.07 m
ρ	0.96	τ_g	0.97
φ_r	40-120^o	α	0.96
$C_R=A_c/A_r$	86	σ_{slope}	0 - 5 mrad
ε_{gi}	0.86	σ_{mirror}	0 - 4 mrad

Computation Procedure

The numerical computation procedure involved solid modelling of the receiver in ANSYS design modeller, discretisation of the receiver in ANSYS meshing and solving the Reynolds averaged Navier-Stokes equations together with the boundary conditions using the finite volume method

implemented in a commercial computational fluid dynamics code, ANSYS Fluent [21]. The computational domain was discretised using hexahedral and quadrilateral elements. Second order upwind scheme ware employed for integrating the governing equations together with the boundary conditions over the computational domain. The SIMPLE algorithm was used for coupling pressure and velocity. Radiation heat transfer in the annulus was modelled using the discrete ordinates model. In order to capture the near wall gradients, the dimensionless wall coordinate y^+ of about 1 was ensured in all simulations. The realisable k- ε model [21] was used for turbulence modelling. The enhanced wall treatment option was used for modelling the near-wall regions. Convergence was obtained with scaled residuals of mass, momentum, turbulent kinetic energy (k) and turbulence dissipation rate (ε) less than 10^{-4} while the energy residuals were less than 10^{-7}. The heat transfer fluid used is sylltherm800 and its properties are temperature dependent as determined from the manufacturer's data sheets. The polynomials used are given in a previous investigation [22].

Validation of Numerical Models

Our numerical results have been validated with data available in literature. The validation of the ray trace results is shown in Figure 3. The same trend exists when compared to the results of Jeter [23], He *et al.* [24] and Yang *et al.* [25]. Good agreement was obtained for the entire range of receiver circumferential angle as shown. LCR is the local concentration ratio, which is the ratio of the actual heat flux on the absorber tube to the incident solar radiation.

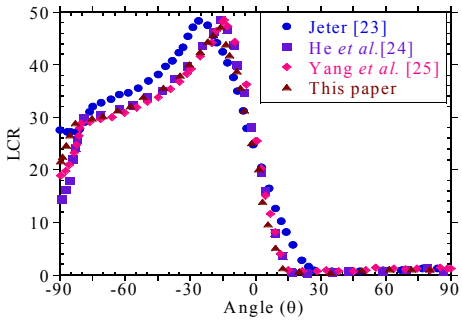

Figure 3 Comparison of present study receiver local concentration ratio with literature

The validation of the thermal performance of the receiver model was done using data from Sandia national laboratories using similar parameters as was used in the experiment [26]. Good agreement was achieved for heat transfer fluid temperature gain and collector efficiency as shown in our previous investigation [22].

RESULTS AND DISCUSIONS

Heat Flux Distribution

For the rim angle of 80° and the concentration ratio of 86 used in this study, the heat flux distribution on the receiver's absorber tube is shown in Figures 4(a) and 4(b) at different slope errors and a specularity errors of 0 mrad and 3 mrad respectively. As shown in the figures, the presence of slope errors significantly affects the heat flux distribution on the receiver's absorber tube. The heat flux peak reduces as the slope error increases. This is because, rays reflected from the reflector are no longer specularly reflected and are rather randomly reflected to different points on the receiver's absorber tube while other rays will miss the receiver tube. The fact that some rays will miss the receiver makes the average heat flux on the absorber tube significantly lower at higher values of slope errors as shown.

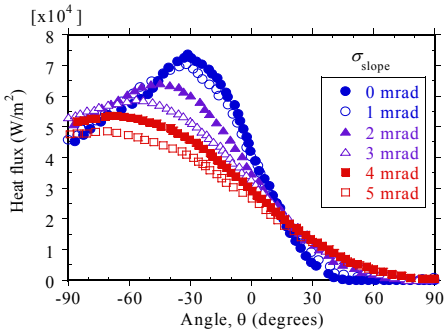

(a)

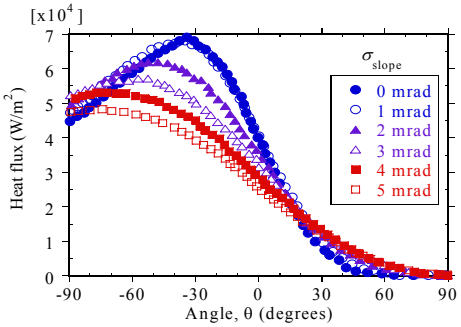

(b)

Figure 4 Heat flux as a function of absorber tube circumferential angle and slope errors for specularity error of: (a) 0 mrad (b) 3 mrad

As shown in Figures 4(a) and Figure 4(b) the variation of heat flux with specularity error is not so significant at the low values of specularity errors considered in this study, but the average heat flux is shown to slightly reduce as the specularity error changes from 0 mrad to 3 mrad. The influence of the specularity error on the heat flux distribution is shown in Figure 5 for a slope error of 3 mrad. As shown, the change in the mirror specularity does not alter the heat flux distribution significantly at any given value of the slope error. However, there is a reduction in the heat flux received by the absorber tube from the reflector especially in areas close to the lower half of the receiver's absorber tube ($-90^o \leq \theta \leq 10^o$). Generally at different combinations of slope errors and specularity errors, the heat flux on the receiver's absorber tube is non-uniform with high heat flux peaks existing at lower values of slope errors.

To characterise the optical performance of the parabolic trough collector system, the optical efficiency given in equation (1) is used. For normal incidence, the remaining factor influencing the optical efficiency is the intercept factor. Figure 6 shows the intercept factor as a function of specularity error

and slope errors. As shown, the intercept factor changes significantly as the slope errors increase. At a specularity error of 0 mrad, the intercept factor reduces by about 21 % as the slope error increases from 0 to 5 mrad. The same reduction is noted at a specularity error of 5 mrad as the slope error increases from 0 to 5 mrad. As shown in the figure, the specularity errors do not significantly affect the intercept factor.

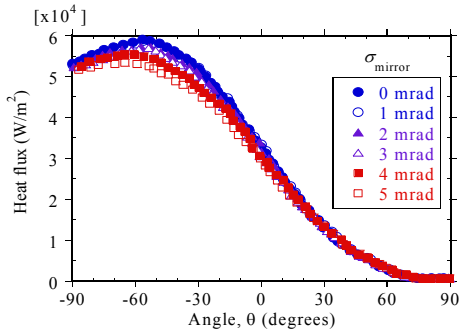

Figure 5 Heat flux as a function of absorber tube circumferential angle and specularity error at a slope error of 3 mrad.

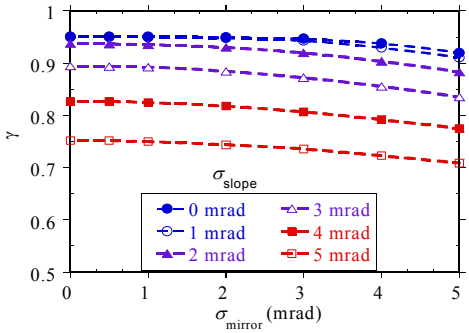

Figure 6 Intercept factor as a function of slope errors and specularity errors.

There is only a slight reduction in the intercept factor as the specularity error increases at a given slope error. For example at a slope error of 3 mrad, the intercept factor reduces by 1% as the specularity error increases from 0 to 2 mrad and by 6 % as the specularity error increases from 0 to 5 mrad. Significant reductions in the intercept factor are noted as the specularity error becomes greater than 4 mrad.

Receiver Thermal Performance

Studies on the thermal performance of parabolic trough receivers have shown that the heat flux distribution on the receiver has a notable effect on the receiver's thermal performance [27]. The heat flux distribution is also expected to affect the temperature distribution in the receiver's absorber tube. Figure 7 shows the temperature distribution in the receiver's absorber tube at a flow rate of 18.5 m^3/h. As shown, the temperature gradients in the receiver's absorber tube are significantly higher at low values of slope errors. This follows from the variation of heat flux with slope errors as shown in Figure 4.

Presence of slope errors reduces the peak heat flux as well as the average heat flux received on the absorber tube, thus low absorber tube temperature gradients as well as average absorber tube temperatures.

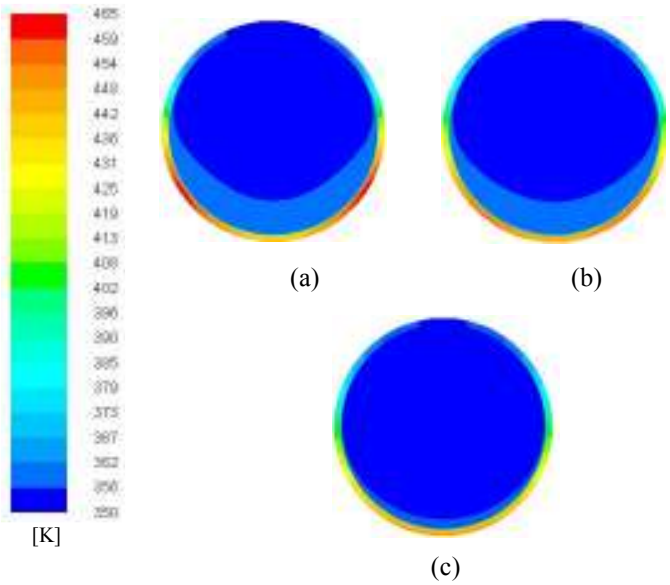

Figure 7 Temperature contours of the absorber tube outlet at a flow rate of 18.5 m^3/h, inlet temperature of 350 K , specularity error of 0 mrad and slope errors of (a) σ_{slope} = 0 mrad, (b) σ_{slope} = 2 mrad, and (c) σ_{slope} = 4 mrad

Figure 8 shows the variation of absorber tube circumferential temperature gradients (difference between maximum and minimum absorber tube temperatures) with Reynolds numbers and slope errors at a temperature of 600 K. The absorber tube circumferential temperature gradients reduce as the slope errors increase. The largest absorber tube circumferential temperature gradients exist at the lowest Reynolds number and lowest slope error of about 184 K when the Reynolds number is 4.5 × 10^4 reducing as the Reynolds numbers increase.

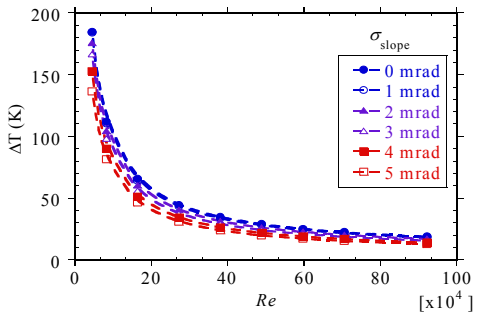

Figure 8 Absorber tube circumferential temperature gradient as a function of Reynolds number and slope error at an inlet temperature of 600 K and specularity error of 0 mrad

Generally, the temperature gradients become lower than 50 K for Reynolds numbers greater than 2.7 × 10^5 at all values of slope errors and specularity errors at an inlet temperature of 600 K. For all the temperatures considered, a flow rate of 30.8 m^3/h ensures temperature gradients less than 50 K a value needed for safe operation of the receiver. The specularity errors are expected to have an insignificant effect on the temperature

gradient since they do not alter the distribution of heat flux on the receiver's absorber tube significantly.

The thermal efficiency of the parabolic trough system is given by equation (6). As the slope errors increase, the useful heat will be affected and therefore the thermal efficiency. Figure 9 shows the thermal efficiency of the parabolic trough system as a function of absorber tube temperature and slope errors.

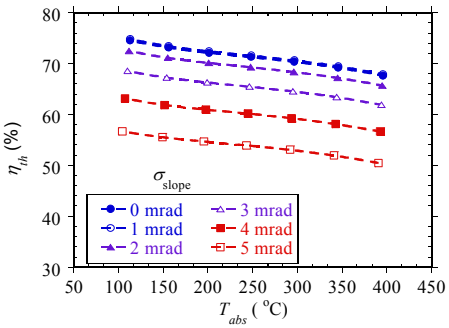

Figure 9 Collector thermal efficiency for a specularity error of 0 mrad as a function of average absorber tube temperature and slope error at a flow rate of 31 m^3/h

As expected, the thermal efficiency reduces as the slope errors increase as shown in the figure. The thermal efficiency is also shown to reduce as the absorber tube temperature increases. This is expected since increased absorber tube temperatures mean increased emissivity of the absorber tube and therefore increased receiver thermal loss. At a given absorber tube temperature or Reynolds number, the thermal efficiency will reduce between 16% - 17% as the slope errors increase from 0 mrad to 5 mrad.

CONCLUSION

In this paper, the influence of slope errors and specularity errors on the optical and thermal performance of a parabolic trough system is presented. Results show that presence of slope errors significantly influences the heat flux distribution on the receiver's absorber tube. The peak heat flux is shown to reduce as the slope errors increase. It is shown that specularity errors do not significantly affect the heat flux distribution, especially values less than 3 mrad. From the study, the intercept factor was found to reduce by about 21% as the slope errors increases from 0 mrad to 5 mrad and by about 5% as specularity errors increases to values above 4 mrad.

The thermal efficiency of the collector was also shown to reduce significantly as the slope errors increased. The thermal efficiency reduces by about 16% – 17% as the slope error increases from 0 to 5 mrad for all values of specularity errors at a given temperature or Reynolds number. The influence of the specularity error on the thermal efficiency was also shown to be small at values of the specularity error lower than 4 mrad.

REFERENCES

[1] Kalogirou S., Solar energy engineering: processes and systems, 1st ed. Oxford, UK, Elsevier Academic Press, 2009.

[2] Price H., Lüpfert E., Kearney D., Zarza E., Cohen G., Gee R., and Mahoney R., Advances in parabolic trough solar power technology, *Journal of Solar Energy Engineering,* Vol. 14, 2002, pp.109-125.

[3] Güven H.M., and Bannerot R.B., Determination of error tolerances for the optical design of parabolic troughs for developing countries, *Journal of Solar Energy*, Vol. 36, 1986, pp.535-550.

[4] Pottler K., Ulmer S., Lüpfert E., Landmann M., Röger M., and Prahl C., Ensuring performance by geometric quality control and specifications for parabolic trough solar fields, *Energy Procedia*, Vol. 49, 2014, pp.2170-2179.

[5] Gaul H., and Rabl A., Incidence-angle modifier and average optical efficiency of parabolic trough collectors, *Transaction of ASME, Journal of Solar Energy Engineering*, Vol.102, 1980, pp.535-550.

[6] Thomas A., and Guven H.M., Effect of optical errors on flux distribution around the absorber tube of a parabolic trough concentrator, *Journal of Energy Conversion and Management*, Vol. 35, 1994, pp.575-582.

[7] Balghouthi M., Ali A.B.H., Trabelsi S.E., and Guizani A., Optical and thermal evaluations of a medium temperature parabolic trough solar collector used in a cooling installation, *Journal of Energy Conversion and Management*, Vol. 86, 2014, pp.1134-1146.

[8] García-Cortés S., Bello-García A., and Ordóñez C., Estimating intercept factor of a parabolic solar trough collector with new supporting structure using off-the-shelf photogrammetric equipment, *Journal of Applied Energy,* Vol. 92, 2012, pp. 815-821.

[9] Lee H., The geometric-optics relation between surface slope error and reflected ray error in solar concentrators, *Journal of Solar Energy* Vol. 101, 2014, pp.299-307.

[10] Maccari A., and Montecchi M., An optical profilometer for the characterisation of parabolic trough solar concentrators. *Journal of Solar Energy*, Vol. 81, 2007, pp.185-194.

[11] Wendelin T., Parabolic trough VSHOT optical characterization in 2005-2006, *Parabolic trough technology workshop*, February 14-16, 2006, Incline Village Nevada.

[12] Lüpfert E., Riffelmann K., Price H., Burkholder F., and Moss T. Experimental analysis of overall thermal properties of parabolic trough receivers, *Journal of Sol Energy Engineering*, Vol. 130, 2008, 021007.

[13] Burkholder F., and Kutscher C., Heat loss testing of Schott's 2008 PTR70 parabolic trough receiver. *NREL Technical Report,* NREL/TP - 550-45633, 2009, pp.1-58.

[14] Burkholder F., and Kutscher C., Heat-loss testing of Solel's UVAC3 parabolic trough receiver, *NREL Technical Repor*t, NREL/TP - 550-42394, 2008, pp.1-19.

[15] SolTrace optical modelling software, NREL, 2012, v.2012.7.9.

[16] Duffie J.A., and Beckman W.A., Solar engineering of thermal processes. 3rd ed. Hoboken, New Jersey, John Wiley and Sons Inc., 2006.

[17] Bendt P., Rabl A., Gaul H.W., and Reed K.A., Optical analysis and optimization of line-focus solar collectors, *Solar Energy Research Institute Report,* SERI/TR 34-092, September 1979, Golden, CO, pp.1-64.

[18] Forristall R., Heat transfer analysis and modeling of a parabolic trough solar receiver implemented in Engineering Equation solver, *NREL Technical Report*, NREL/TP-550-34169, October 2003, pp.1-145.

[19] García-Valladares O., and Velázquez N., Numerical simulation of parabolic trough solar collector: Improvement using counter flow concentric circular heat exchangers, *International Journal of Heat Mass Transfer*, Vol. 52, 2009, pp.597-609.

[20] Mullick S.C., and Nanda S.K., An improved technique for computing the heat loss factor of a tubular absorber, *Journal of Solar Energy*, Vol. 42, 1989, pp.1-7.

[21] ANSYS® Academic research, release 14.5, ANSYS FLUENT user's guide, ANSYS, Inc.

[22] Mwesigye A., Bello-Ochende T., and Meyer J.P., Numerical investigation of entropy generation in a parabolic trough receiver at different concentration ratios, *Journal of Energy,* Vol. 53, 2013, pp.114-127.

[23] Jeter S.M., Calculation of the concentrated flux density distribution in parabolic trough collectors by a semifinite formulation, *Journal of Solar Energy*, Vol. 37, 1986, pp.335-345.

[24] He Y., Xiao J., Cheng Z., and Tao Y., A MCRT and FVM coupled simulation method for energy conversion process in parabolic trough solar collector, *Journal of Renewable Energy,* Vol.36, 2011, pp.976-985.

[25] Yang B., Zhao J., Xu T., and Zhu Q., Calculation of the concentrated flux density distribution in parabolic trough solar concentrators by Monte Carlo ray-trace method, *Journal of Photonics and Optoelectronic (SOPO,* 2010, pp.1-4.

[26] Dudley E.V., Kolb J.G., Mahoney A.R., Mancini T.R.., Sloan M., and Kearney D., Test results: SEGS LS-2 solar collector, *Sandia National Laboratory* SAND94-1884,1994.

[27] Mwesigye A., Bello-Ochende T., and Meyer J.P., Minimum entropy generation due to heat transfer and fluid friction in a parabolic trough receiver with non-uniform heat flux at different rim angles and concentration ratios, *Journal of Energy*, Vol.73, 2014, pp.606-617.